Non-Brownian Microrheology of a Fluid-Gel Interface

E. K. Hobbie,[1] S. Lin-Gibson,[1] and S. Kumar[2]

[1]*Polymers Division, National Institute of Standards and Technology, Gaithersburg, Maryland 20899, USA*

[2]*Department of Chemical Engineering and Materials Science, University of Minnesota, Minneapolis, Minnesota 55455, USA*

(Received 27 July 2007; published 20 February 2008)

We use stroboscopic video microscopy to study the motion of a sheared fluid-gel interface. Mechanical noise plays a role analogous to temperature, but with a low-frequency breakdown of linear response consistent with an underlying instability. We relate the fast motion of the interface to the rheological properties of the gel, laying the foundation for a non-Brownian optical microrheology.

DOI: 10.1103/PhysRevLett.100.076001 PACS numbers: 83.85.Ei, 47.20.Ma, 83.60.Bc

Fluid flow near a deformable solid is ubiquitous in nature and technology. Blood flow through vessels [1], lubrication of cartilage in joints [2], microfluidic valves [3], and coating and printing processes [4] are all examples of systems governed by the interaction between a flowing fluid and an elastic solid. Similar interfacial phenomena also occur in the multiphase flow of complex fluids [5–9]. Although the rheological properties of such nonequilibrium interfaces are both important and intriguing, they are inaccessible to conventional rheometry, creating the need for new noninvasive and localized techniques.

Optical microrheology has recently emerged as a powerful tool in condensed matter and biological physics [10]. Passive microrheology relies on thermal fluctuations to excite optical signal and has recently been extended to interfaces [11–14]. Active microrheology uses externally applied forces to achieve the same end [15–17], with the potential to be applied at the interface between a flowing fluid and an elastic solid. For sufficiently soft solids, however, the situation is complicated by the free location of the fluid-solid interface, which can give rise to nonlinear behavior and *elastohydrodynamic* instabilities [7,18]. The simplest example of such an instability occurs when a viscous fluid flows past a polymer gel. Linear stability analysis predicts that even in the absence of inertia, the interface will become unstable to periodic undulations when the ratio of viscous to elastic forces, $\Gamma = v\eta/RE$, exceeds a critical value [19], where v is a characteristic fluid velocity, R is a characteristic length scale, η is the fluid viscosity, and E is the shear modulus of the gel.

Here, we measure the motion of a sheared fluid-gel interface for which mechanical noise plays a role analogous to temperature. We find a low-frequency breakdown of linear response consistent with an underlying instability, but by focusing on the fast motion, we recover linear response, laying the foundation for a particular type of non-Brownian optical microrheology that can be used to extract the bulk viscoelasticity of an otherwise inaccessible soft solid from the dynamics of a sheared interface.

A schematic of the experiment is shown in Fig. 1. A polydimethylsiloxane (PDMS) gel of thickness h_g was prepared on the lower plate of an optical shear cell. A portion of the gel was also prepared on a disposable plate to independently monitor the dynamic shear modulus, $G^*(\omega) = G'(\omega) + iG''(\omega)$, in a controlled-strain rheometer. To form the gels, dimethylvinyl-terminated dimethyl siloxane oligomer was reacted with a cross-linker (trimethylsiloxy terminated methylhydrosiloxane-dimethylsiloxane copolymer). An organoplatinum catalyst and diallyl maleate inhibitor were added to achieve the appropriate room-temperature processing window. By varying the ratio of oligomer to cross-linker, we study the interval 20 Pa $< E <$ 10^3 Pa.

After the gel cured, a dilute suspension of 3 μm latex spheres in ethanol was introduced onto the gel surface at a point of observation 2 cm from the center of the 4 cm radius plates. When the ethanol evaporates, the spheres adhere to the interface, and a Newtonian fluid of polypropylene glycol (PPG, $M_w = 4000$, $\eta = 1$ Pa s) was poured over the gel. The top plate was then lowered to a final fluid thickness h_f. For the data presented here, h_g was *ca.* 0.5 cm with 100 μm $< h_f <$ 1500 μm. Shear flow of mean local shear rate $\dot{\gamma}$ (from 0.1 s^{-1} to 10 s^{-1}) was introduced through a motor-driven rotation of the top plate. The Reynolds number, $\mathrm{Re} = \rho\dot{\gamma}h_f^2/\eta$ where ρ is the PPG density, is <0.025. After stepping the fluid to $\dot{\gamma}$, the interface was monitored optically until it reached a steady state. The motion was then stroboscopically recorded (45 μs flash) and analyzed using standard techniques of digital

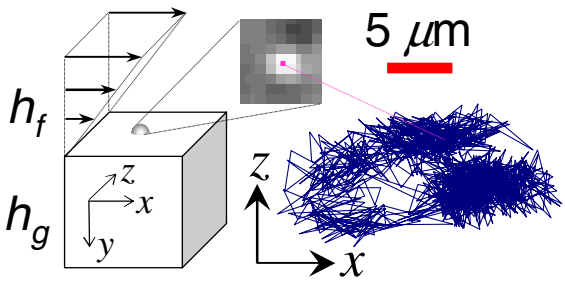

FIG. 1 (color online). Schematic of the experiment showing 2D motion characteristic of a 344 Pa gel at $\dot{\gamma} = 10$ s^{-1}.

video microscopy [20]. In all cases, the motion of the interface at the point of observation occurs in the focal plane of flow (x) and vorticity (z). Tracking the trajectories of neighboring spheres further reveals that this motion is coherent over *ca.* 10^3 μm, with the interface at the observation point moving as a rigid body, and single-particle tracking is thus sufficient.

The quiescent interface is static, implying that external noise is critical. Indeed, measured 2D interfacial trajectories are stochastic in appearance (Fig. 1), reminiscent of a trapped Brownian particle, even though the system is completely non-Brownian. External noise can be characterized as either nonshearing or shearing, where the former arises from the coherent vibration of both plates and the latter arises from their relative motion. To characterize nonshearing noise, we tracked adhered microspheres in the absence of any fluid as a function of motor speed and gel modulus with the top plate above the gel-air interface. This motion varied from $<9\%$ ($\dot{\gamma} = 0.1$ s^{-1}) to $<1\%$ ($\dot{\gamma} = 10$ s^{-1}) of that observed under the same conditions with the fluid in place. Shearing noise, on the other hand, is the dominant source of signal. It arises from either "fast" variations in the speed of the top plate (motor) or "slow" variations in the separation of the plates (wobble). Wobble, measured optically to be ± 2 μm, leads to slow periodic noise. Motor noise excites fast signal and is measured by optically tracking objects fixed to the top plate. It consists of a dominant harmonic on a stochastic background. The Nyquist frequency for our standard video acquisition is 100 rad/s, above which the periodic part of the fast driving signal will be aliased.

In Fig. 2, we show a comparison of the measured interfacial motion for gels of two different E (28 and 344 Pa) at the same shear rate (5 s^{-1}). As expected, the softer gel shows larger fluctuations, with a component of large-amplitude motion in the softer gel being markedly slower [Fig. 2(a)]. The lower panel of Fig. 2(a) shows an expanded time interval for the softer gel. Taking the time derivative of the displacement gives velocity [Fig. 2(b)], the lower panel again highlighting the fast motion of the softer gel. Continuity of tangential shear stress across the interface implies that these velocity fluctuations are essentially variations in stress, the data further suggesting that such fluctuations occur predominantly along the direction of flow. Accounting for viscous penetration in the fluid, the measured interfacial velocity fluctuations are comparable to those expected in an unbounded fluid at a depth corresponding to the position of the interface based on measured variations in the speed of the top plate (Fig. 2, lower right panel, 34 s to 35 s).

The mean-square displacement (MSD) of the interface around steady-state equilibrium as a function of time is shown in Fig. 3(a) for a 28 Pa gel at 10 s^{-1}. The motion appears "diffusive" at early t and "caged" with a slow periodic component at later t, where the slow period is due to wobble. A high-frequency harmonic in the speed of the top plate is also evident in the z-component of the MSD. Assuming linear viscoelasticity, we can compute the effect of wobble on the displacement since all of the parameters are known *a priori*. Such a comparison [inset Fig. 3(a), $t > 0$] suggests a breakdown of linear response in the amplitude of the slow periodic motion. The data also suggest intermittent slow aperiodic behavior [inset Fig. 3(a), $t < 0$], further evidence for the importance of nonlinear effects

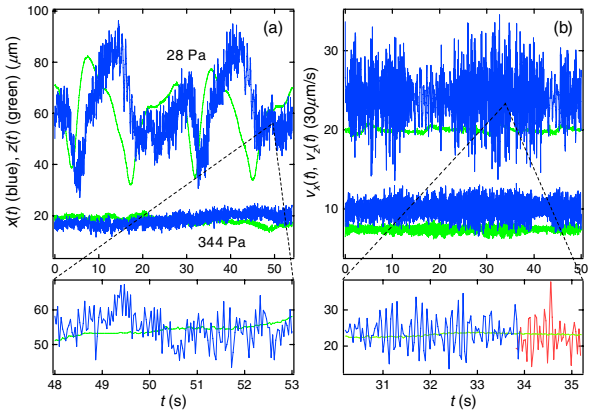

FIG. 2 (color online). (a) Fluctuations in x and z as a function of t at $\dot{\gamma} = 5$ s^{-1} for $E = 28$ and 344 Pa, where the dark (light) curves denote x (z). The lower panel shows the response of the 28 Pa gel at faster timescales. (b) Velocity fluctuations from (a), where the lower panel again shows the response of the 28 Pa gel at faster time scales. Imposed velocity fluctuations based on the measured motion of the top plate are indicated in the lower right panel. All curves are offset for clarity.

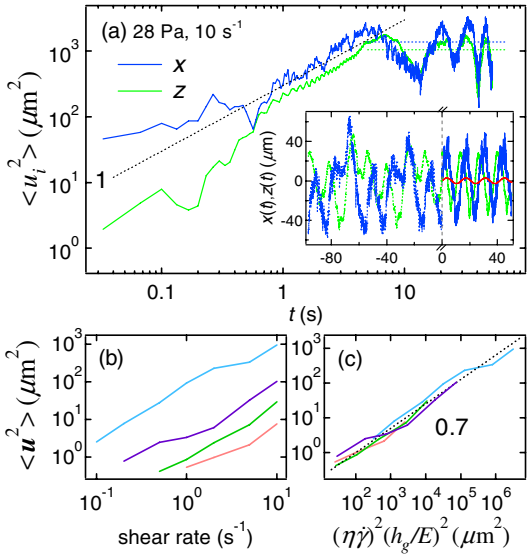

FIG. 3 (color online). (a) Log-log plot of the MSD vs t along x (dark) and z (light) for $E = 28$ Pa at $\dot{\gamma} = 10$ s^{-1}, where the inset shows typical steady-state displacement for two temporally separated intervals [delineated $t < 0$ and $t > 0$] with the linear response for plate wobble (smooth sinusoid). (b) Steady-state MSD in the x-z plane vs $\dot{\gamma}$ for different E (28 Pa, 110 Pa, 344 Pa, and 990 Pa from top to bottom) with scaling (c) as described in the text.

at low-frequency. The steady state MSD as a function of $\dot{\gamma}$ for different E is shown in Fig. 3(b). Taking the mean strain of fluctuations as $\sqrt{\langle \boldsymbol{u}^2 \rangle}/h_g$ and assuming that the magnitude of stress fluctuations is $\lambda \eta \dot{\gamma}$—with $\lambda \simeq 0.1$ being a dimensionless constant characterizing the effective strength of the noise—balancing stress at the interface gives $\langle \boldsymbol{u}^2 \rangle \propto (\eta \dot{\gamma})^2 (h_g/E)^2$ [Fig. 3(c)]. This simple force balance argument (which neglects boundary conditions, nonlinear effects, and viscous loss) predicts a slope of 1 in Fig. 3(c), with the data suggesting an exponent of 0.7. The scaling enables an empirical determination of E from the measured MSD.

On a more quantitative level, a useful point of reference is the inertialess flow of a Newtonian fluid past a flat linear elastic solid. When the shear is turned on, the interface relaxes exponentially to a new equilibrium position dictated by force balance, with a characteristic time scale $\tau = (h_g/h_f)(\eta/E)$. In the absence of noise, there are no fluctuations, and we thus consider the steady-state 2D displacement, $\boldsymbol{u}(t)$, in response to externally imposed 2D vector stress fluctuations, $\boldsymbol{\sigma}(t)$, of zero mean and unspecified correlation, for which

$$\dot{\boldsymbol{u}} + \boldsymbol{u}/\tau = (h_f/\eta)\boldsymbol{\sigma}(t), \tag{1}$$

with $\boldsymbol{u}(0) = 0$. This has the general solution

$$\boldsymbol{u}(t) = (h_f/\eta) \int_0^t e^{-(t-t')/\tau} \boldsymbol{\sigma}(t') dt' \tag{2}$$

from which we obtain the mean-square displacement

$$\langle \boldsymbol{u}^2(t) \rangle = (h_f/\eta)^2 \int_0^t \int_0^t e^{(t'+t''-2t)/\tau} \langle \boldsymbol{\sigma}(t') \cdot \boldsymbol{\sigma}(t'') \rangle dt' dt'' \tag{3}$$

for a point on the interface. Taking the Fourier transform of Eq. (2) gives $\boldsymbol{u}(\omega) = h_g \boldsymbol{\sigma}(\omega)/G^*(\omega)$ with $G^*(\omega) = E(1 + i\omega\tau)$, all of the loss in our simplified model arising from viscous damping in the fluid. This expression is generalized by identifying $G^*(\omega)$ as the shear modulus of the gel [21]. If non-Brownian stress fluctuations at the interface satisfy a form of the fluctuation-dissipation theorem [22], with $\langle |\sigma_i(\omega)|^2 \rangle = 2\alpha_i(\dot{\gamma}) G''(\omega)/\omega$, then the power spectrum of displacements is

$$\langle |u_i(\omega)|^2 \rangle = \frac{2\alpha_i h_g^2 G''(\omega)}{\omega |G|^2}, \tag{4}$$

where the noise strength $\alpha_i(\dot{\gamma})$ is taken to be anisotropic in the x-z plane.

The measured power spectra of steady-state displacement fluctuations for a 28 Pa gel at varied $\dot{\gamma}$ are shown in Fig. 4. The peak labeled A corresponds to wobble, while B and its subharmonics reflect the fast periodic component of the driving force. If the stress correlator in Eq. (3) is a delta function, our simple model heuristically satisfies the functional form of the fluctuation-dissipation theorem, with the ω^{-2} power law representing the high-frequency limit of

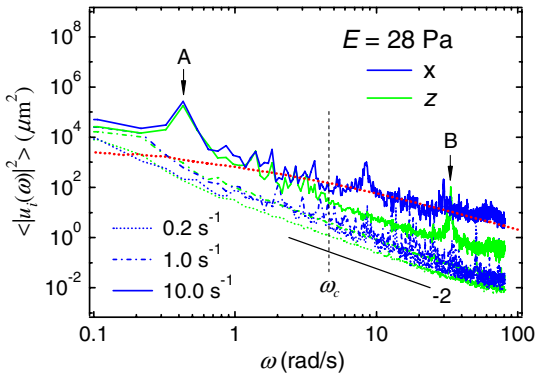

FIG. 4 (color online). Power spectra of displacement fluctuations for a 28 Pa gel, where the dark (light) curve denotes x (z). The the smooth dashed curve for 10 s^{-1} is the profile calculated from Eq. (4) using $G^*(\omega)$ from bulk rheology. Frequencies corresponding to small variations in the gap (a) and the periodic part of the fast driving force (b) at 10 s^{-1} are indicated, as is the cutoff frequency used to distinguish fast and slow modes.

Eq. (4). The general validity of such an approach for the strongly driven interface can be queried by using $G^*(\omega)$ independently measured with bulk rheometry in Eq. (4), and such a comparison (smooth dashed curve, Fig. 4) supports the scenario of harmonics of the driving frequency superposed on a dominant ''thermal'' background. The power spectra also suggest a breakdown of linear response at low frequency, where the data deviate from the profile of Eq. (4). This is consistent with the behavior shown in Fig. 3, and it complicates any attempt to extract the gel viscoelasticity from the motion of the sheared interface. As the higher frequency modes are more intimately linked to linear response, we thus propose filtering out the low-frequency motion before further analysis of the MSD. To delineate fast modes from ''slow'' modes, we introduce the cutoff frequency ω_c shown in Fig. 4, which corresponds to the degree of filtering needed to remove the majority of the z-component of motion (Fig. 4). It also coincides with the characteristic frequency where the buckling instability is expected to emerge for the soft gels [4,18,19]. Filtering was performed by Fourier transforming the 2D trajectories to the frequency domain, multiplying the complex amplitude by the step function $\theta(\omega - \omega_c)$, and then transforming back to the time domain.

Filtered MSD data for two different gels at $\dot{\gamma} = 10$ s^{-1} (using the same ω_c) are shown in Fig. 5(a). The effect of filtering can be seen by comparing the 28 Pa data in Fig. 5(a) with that in Fig. 3(a). In both cases, the motion sinusoidally relaxes to a plateau. When the stress correlator in Eq. (3) is a delta function, the MSD relaxes exponentially. For harmonic correlation, however, the relaxation contains a damped oscillation with the same decay time. A fit of the filtered MSD to a sum of these two effects [sinusoidal curves, Fig. 5(a)] requires different damping for each, implying that the periodic oscillations appear

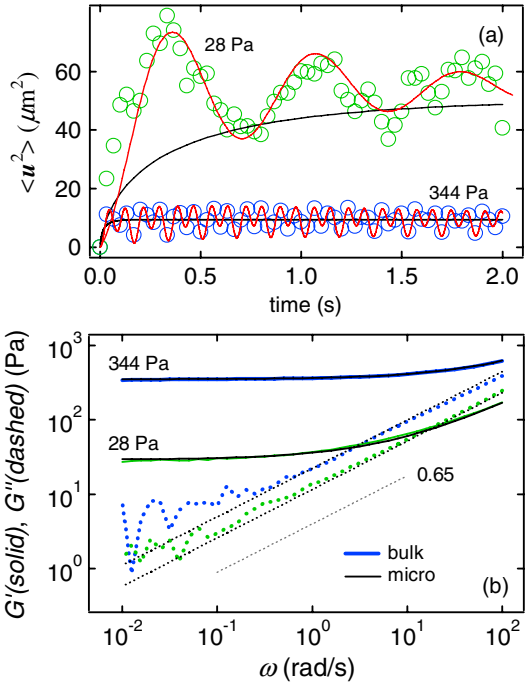

FIG. 5 (color online). (a) Filtered MSD for a "soft" and "hard" gel driven at 10 s^{-1}. The sinusoidal curves are from Eq. (3), where the response of the 28 Pa gel contains one harmonic and that of the 344 Pa gel contains two. The smooth black curves are stretched-exponential relaxations motivated by the bulk rheological response. (b) Comparison of the measured bulk rheology with that based on the smooth fits in (a).

underdamped. Focusing instead on the underlying smooth relaxation, we know from bulk rheology that loss in the gels actually scales as $\omega^{-0.65}$, and we thus model the envelope of the filtered MSD using a stretched exponential relaxation with an exponent of 0.65 [smooth black curves, Fig. 5(a)] to account for the broad range of linear relaxation rates in the gel. Taking the numerical Laplace transform of these expressions, we empirically adopt the approach of Brownian microrheology [10,11] to obtain the viscoelastic shear modulus of the gel by analytically continuing $G^{-1}(s) \propto s\langle \boldsymbol{u}^2(s)\rangle$ via $s \rightarrow i\omega$, as shown in Fig. 5(b). In this comparison, the shape of $G^*(\omega)$ is dictated by the amplitude and decay constant of the smooth stretched-exponential relaxations in Fig. 5(a), with a single multiplicative factor reflecting the strength of the non-Brownian noise. The comparison in Fig. 5(b) is obtained by varying the fits in Fig. 5(a) to optimize the agreement between the bulk and micro results.

What we describe here represents a novel form of active bulk microrheology, but it appears to be somewhat limited by the instability of the sheared interface. The two types of external noise encountered are exemplary of what one would expect in any rotating plate device. Geometry-specific boundary conditions are likely critical, and buckling of the interface at the outer constrained edge of the gel—linked to strain fields in both the vorticity and gradient directions—would give rise to a z-component of motion at the point of observation for the rotating parallel-plate scenario in question here. A perturbative treatment that connects the low-frequency nonlinear response to the linear viscoelasticity of the gel for different boundary conditions in the presence of noise of varying frequency would be quite useful in this regard, and we hope that the work described will help inspire such an effort.

We thank S. Hudson, H. Hua, K. Migler, G. McKinley, J. Gollub, J. Israelachvili, R. Hobbie, and S. Roberts for useful discussions. S. K. acknowledges support from the ACS-PRF.

[1] P. Alstrom *et al.*, Phys. Rev. Lett. **82**, 1995 (1999).
[2] J. M. Skotheim and L. Mahadevan, Phys. Rev. Lett. **92**, 245509 (2004); Phys. Fluids **17**, 092101 (2005).
[3] S. R. Quake and A. Scherer, Science **290**, 1536 (2000).
[4] X. Yin and S. Kumar, Phys. Fluids **17**, 063101 (2005).
[5] S. M. Fielding and P. D. Olmsted, Phys. Rev. Lett. **96**, 104502 (2006).
[6] R. Ganapathy and A. K. Sood, Phys. Rev. Lett. **96**, 108301 (2006).
[7] M. D. Eggert and S. Kumar, J. Colloid Interface Sci. **278**, 234 (2004); V. Gkanis and S. Kumar, Phys. Fluids **15**, 2864 (2003).
[8] I. Cohen *et al.*, Phys. Rev. Lett. **97**, 215502 (2006).
[9] J. F. Gilchrist and J. M. Ottino, Phys. Rev. E **68**, 061303 (2003).
[10] T. A. Waigh, Rep. Prog. Phys. **68**, 685 (2005).
[11] T. G. Mason and D. A. Weitz, Phys. Rev. Lett. **74**, 1250 (1995).
[12] V. Prasad, S. A. Koehler, and E. R. Weeks, Phys. Rev. Lett. **97**, 176001 (2006).
[13] J. Wu and L. L. Dai, Appl. Phys. Lett. **89**, 094107 (2006); Langmuir **23**, 4324 (2007).
[14] A. J. Levine, T. B. Liverpool, and F. C. MacKintosh, Phys. Rev. Lett. **93**, 038102 (2004); A. J. Levine and F. C. MacKintosh, Phys. Rev. E **66**, 061606 (2002).
[15] J. P. Pantina and E. M. Furst, Phys. Rev. Lett. **94**, 138301 (2005).
[16] T. M. Squires and J. F. Brady, Phys. Fluids **17**, 073101 (2005).
[17] A. Anguelouch, R. L. Leheny, and D. H. Reich, Appl. Phys. Lett. **89**, 111914 (2006).
[18] V. Kumaran and R. Muralikrishnan, Phys. Rev. Lett. **84**, 3310 (2000); Phys. Fluids **14**, 775 (2002); V. Shankar and V. Kumaran, J. Fluid Mech. **434**, 337 (2001).
[19] V. Kumaran, G. H. Fredrickson, and P. Pincus, J. Phys. II (France) **4**, 893 (1994).
[20] T. Savin and P. S. Doyle, Biophys. J. **88**, 623 (2005).
[21] $G''(\omega) > \eta\omega$ and the dominant source of loss is the gel.
[22] G. D'Anna *et al.*, Nature (London) **424**, 909 (2003).